# Mechanism of Homogeneous Reduction of CO$_2$ by Pyridine: Proton Relay in Aqueous Solvent and Aromatic Stabilization

Chern-Hooi Lim,[†] Aaron M. Holder,[†,‡] and Charles B. Musgrave*[,†,‡]

[†]Department of Chemical and Biological Engineering and [‡]Department of Chemistry and Biochemistry, University of Colorado at Boulder, Boulder, Colorado 80309, United States

Ⓦ *Web-Enhanced Feature* Ⓢ *Supporting Information*

ABSTRACT: We employ quantum chemical calculations to investigate the mechanism of homogeneous CO$_2$ reduction by pyridine (Py) in the Py/p-GaP system. We find that CO$_2$ reduction by Py commences with PyCOOH^0 formation where: (a) protonated Py (PyH$^+$) is reduced to PyH^0, (b) PyH^0 then reduces CO$_2$ by one electron transfer (ET) via nucleophilic attack by its N lone pair on the C of CO$_2$, and finally (c) proton transfer (PT) from PyH^0 to CO$_2$ produces PyCOOH^0. The predicted enthalpic barrier for this proton-coupled ET (PCET) reaction is 45.7 kcal/mol for direct PT from PyH^0 to CO$_2$. However, when PT is mediated by one to three water molecules acting as a proton relay, the barrier decreases to 29.5, 20.4, and 18.5 kcal/mol, respectively. The water proton relay reduces strain in the transition state (TS) and facilitates more complete ET. For PT mediated by a three water molecule proton relay, adding water molecules to explicitly solvate the core reaction system reduces the barrier to 13.6−16.5 kcal/mol, depending on the number and configuration of the solvating waters. This agrees with the experimentally determined barrier of 16.5 ± 2.4 kcal/mol. We calculate a pK_a for PyH^0 of 31 indicating that PT preceding ET is highly unfavorable. Moreover, we demonstrate that ET precedes PT in PyCOOH^0 formation, confirming PyH^0's pK_a as irrelevant for predicting PT from PyH^0 to CO$_2$. Furthermore, we calculate adiabatic electron affinities in aqueous solvent for CO$_2$, Py, and Py·CO$_2$ of 47.4, 37.9, and 66.3 kcal/mol respectively, indicating that the anionic complex PyCOO$^-$ stabilizes the anionic radicals CO$_2^-$ and Py$^-$ to facilitate low barrier ET. As the reduction of CO$_2$ proceeds through ET and then PT, the pyridine ring becomes aromatic, and thus Py catalyzes CO$_2$ reduction by stabilizing the PCET TS and the PyCOOH^0 product through aromatic resonance stabilization. Our results suggest that Py catalyzes the homogeneous reductions of formic acid and formaldehyde en route to formation of CH$_3$OH through a series of one-electron reductions analogous to the PCET reduction of CO$_2$ examined here, where the electrode only acts to reduce PyH$^+$ to PyH^0.
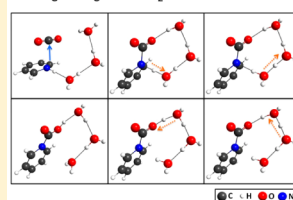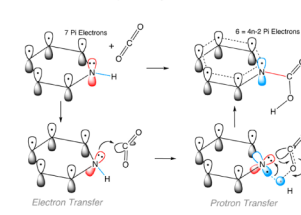
1. INTRODUCTION

Growing concern over the concentration of CO$_2$ in the atmosphere has motivated efforts to explore approaches to reduce the level of atmospheric CO$_2$.[1−3] One well-known proposal involves CO$_2$ sequestration and storage, which faces a number of difficult practical challenges including cost, efficiency, sustainability, and safety.[4−8] Another possible approach involves chemical reduction of CO$_2$ into fuels, such as methanol (CH$_3$OH),[9−13] or C$_n$ ($n \geq 2$) products, such as polyethylene.[3,14] Despite its enormous potential benefits, efficient chemical conversion of CO$_2$ into useful reduced species remains a formidable challenge due to the thermodynamic and kinetic stability of CO$_2$ in its highly oxidized form.

Several chemical approaches have been explored in attempts to reduce CO$_2$ to CH$_3$OH, including homogeneous,[15−21] heterogeneous,[22−24] electrochemical,[25−27] photochemical,[28−31] and photoelectrochemical (PEC) reactions.[14,32−38] PEC approaches show particularly significant promise because they can directly use sunlight as the renewable energy source to reduce CO$_2$. One especially intriguing PEC approach was discovered by Bocarsly et al. in 2008.[39] This system involves the

use of pyridine (Py), which is suggested to undergo protonation to pyridinium (PyH$^+$) in acidic aqueous solutions and act as an electron transfer (ET) mediator that is electrochemically reduced to the pyridinium radical (PyH^0) at a photoexcited p-type GaP electrode surface with an indirect bandgap of 2.24 eV.[39] PyH^0 has been proposed to act as the active catalyst that chemically reduces CO$_2$ to CH$_3$OH.[39−41] Although many details of the mechanism of CO$_2$ reduction by this system remain unknown, it is one of the most efficient PEC systems in reducing CO$_2$, converting CO$_2$ to CH$_3$OH at near 100% Faradaic efficiency at underpotentials ~300 mV below the standard potential of −0.52 V vs SCE at a pH of 5.2.[39] PyH$^+$ was also observed to be electrochemically reduced by a Pd cathode and to subsequently reduce CO$_2$ to CH$_3$OH at an overpotential of ~200 mV.[42]

In 2010 Bocarsly et al. reported experimentally derived mechanistic steps for the reduction of CO$_2$ by PyH^0, which they proposed occurs in the homogeneous phase.[40] However,

Keith et al. argue that PyH^0 cannot be the active species that chemically reduces CO_2 in the homogeneous phase[43] based on their calculated homogeneous standard reduction potential (E^0) for PyH^+ of -1.47 V vs SCE, which is -0.9 V more negative than the -0.58 V experimental value measured on a Pt electrode.[40] Thus, they conclude that PyH^0 should not be formed at $E^0 = -0.58$ V and proceed to chemically reduce CO_2.[43] Their calculated E^0 agrees with the homogeneous PyH^+ reduction potentials calculated by ourselves (-1.31 V) and Tossell (-1.44 V).[44]

Because electrochemical reduction of PyH^+ is a highly surface-dependent process,[40,45] experimentally measured reduction potentials on various electrode surfaces may deviate from calculated E^0's that assume a homogeneous process absent of surface effects. For example, in 1979 Yasukouchi et al. concluded that the PyH^+/PyH^0 reduction potential "at various metals (Pt, Pd, Au, Ti, Fe, Ni, Cd, Pb, Hg, etc.), on the whole, shifted to more negative potentials from platinum to mercury in the order similar to that of the well-known hydrogen overvoltage".[45] For instance, on Pt the peak potential, $E_p(PyH^+/PyH^0)$, is -0.41 V vs SCE (-0.75 V vs Ag/AgClO$_4$), which is consistent with $E^0 = -0.58$ V vs SCE measured by Bocarsly et al.[40] In contrast, on a dropping mercury electrode the measured -1.19 V vs SCE (-1.53 V vs Ag/AgClO$_4$) reduction half-wave potential approaches the calculated homogeneous E^0, which we propose results from diminishing surface effects of the Hg electrode on PyH^+ reduction. Conservation of energy dictates that the decreased reduction potential of PyH^+ exhibited on several surfaces, including Pt[40] and Pd,[42] must be accounted for by endothermic PyH^0 desorption, which may be overcome thermally or by applied overpotentials. Specifically, at least 16.8 kcal/mol or -0.73 V (the difference between the calculated homogeneous E^0 of -1.31 V and the experimentally measured -0.58 V) is required to produce PyH^0 in the homogeneous phase.

A number of experiments have demonstrated the surface-mediated reduction of PyH^+ to PyH^0, which then desorbs from the electrode and diffuses into the homogeneous phase.[39–42,45–48] Yasukouchi et al. showed that peak currents in cyclic voltammograms (CVs) (a) varied linearly with acid concentration at constant Py concentration and (b) varied linearly with Py concentration at constant acid concentration, confirming that the protonated species PyH^+ is reduced to PyH^0.[45] These results are consistent with measurements performed independently by Bocarsly et al. in 1994 where at an electrolyte pH > 7 "no cyclic voltammetric features associated with pyridine are observed, indicating that the electroactive species is the protonated pyridinium cation".[42] The linear dependence of peak current on PyH^+ concentration shown by Yasukouchi et al. rules out the reduction of dimeric derivatives of PyH^+, such as the 4,4′-bipyridine dimer suggested by Keith et al.,[43] in agreement with Bocarsly et al.'s experimental observation that no Py is consumed to form dimers.[42] Furthermore, the oxidation current in CVs observed when the potential scan was reversed indicates PyH^0 in the homogeneous phase.[40,42,45] Finally, in the PEC experiment performed by Bocarsly et al., in addition to illumination of the p-GaP electrode, a negative electrical bias was applied.[39] Under these conditions the p-GaP electrode should possess a reduction potential significantly above the homogeneous E^0 of PyH^+ (-1.31 V), assuming that the conduction band edge of p-GaP is above the LUMO of PyH^+. Thus, PyH^0 should exist in the aqueous phase to homogeneously catalyze CO_2 reduction.

To further elucidate the surface dependence of PyH^+ electrochemical reduction we have performed calculations of PyH^+ adsorption on a water-solvated unbiased Pt(111) surface (see Supporting Information (SI), section 1). Our calculations predict a strong binding interaction of PyH^+ with the electrode surface resulting in an adsorption energy of 1.0 eV/molecule on Pt(111). The strong binding energy of PyH^+ to the electrode surface is evident by the significant mixing of the adsorbate and surface states. This leads to broadening of the PyH^+ LUMO upon adsorption, resulting in transfer of $0.56e^-$ from Pt to PyH^+ and disruption of the aromaticity of PyH^+. Consequently, the strong binding interaction of heterocyclic aromatic[49] PyH^+ with Pt(111) significantly lowers (becomes less negative) its heterogeneous reduction potential,[50] explaining the discrepancy between the experimentally measured heterogeneous E^0 and calculated homogeneous E^0 for PyH^+.

Keith et al. suggested that even if PyH^0 was formed it would not catalyze CO_2 reduction due to the difficulty in deprotonating the reduced species, based on their calculated pK_a for PyH^0 of $\sim$27.[43] Although we calculate a similar pK_a for PyH^0 of $\sim$31, we predict that PyH^0's pK_a does not indicate the reactivity of PyH^0 toward CO_2 reduction because, as we show, ET from PyH^0 to CO_2 precedes proton transfer (PT), which effectively lowers the pK_a of the partially oxidized PyH^0 species. Our results demonstrate that the electrochemically produced PyH^0 reacts with CO_2 in the homogeneous phase to form the carbamate species $PyCOOH^0$, consistent with the EC′ mechanism[50] previously proposed by Bocarsly et al.[40,41] Furthermore, our calculated enthalpic barrier agrees with Bocarsly's experimentally determined barrier of 16.5 ± 2.4 kcal/mol.[41] We predict that two effects significantly lower the barrier for this process: (1) water molecules play a central role in facilitating $PyCOOH^0$ formation by solvent-assisted proton-coupled electron transfer (PCET) where ET precedes PT and (2) aromatic stabilization leads to the production of the low-energy one e^- transfer product ($PyCOO^-$) to significantly lower the barrier for this process.

This contribution focuses on predicting a detailed mechanism of CO_2 reduction in the Py/p-GaP system with associated energetics and providing a thorough understanding of the intriguing effects that underlie the homogeneous reduction of CO_2 by PyH^0 to form $PyCOOH^0$. In particular, we attempt to answer several fundamental questions related to CO_2 reduction in this system. These include: (i) Is CO_2 reduced through one e^- or two e^- transfers? (ii) If CO_2 reduction proceeds through one e^- transfer as proposed by Bocarsly et al.,[40] how does Py act as a catalyst to stabilize the high-energy CO_2^- anionic radical ($E^0_{exp} = -2.18$ V vs SCE)?[51] (iii) Is ET and PT from PyH^0 to CO_2 stepwise or concurrent? (iv) If ET and PT occur sequentially, does ET precede PT or vice versa? Finally, (v) Is CO_2 prebent to lower its reorganization energy for ET from PyH^0, and is prebending of CO_2 a general requirement for facile ET and thus an efficient reduction process?

Formation of the $PyCOOH^0$ carbamate species has been identified as an important intermediate, and its production has been proposed to be the rate-determining step for the reduction of CO_2 to CH_3OH.[40,41] Scheme 1 shows two potential homogeneous routes to $PyCOOH^0$ formation.[40] Route 1 begins with the protonation of Py to form PyH^+. PyH^+ is then reduced at the p-GaP surface by a photoexcited electron to form PyH^0, which then diffuses into solution from the electrode. PyH^0 then reacts with CO_2 to form $PyCOOH^0$ in the homogeneous phase, which becomes further reduced into

Scheme 1. Two Potential Routes for the Formation of PyCOOH[0] in the Homogeneous Phase[a]
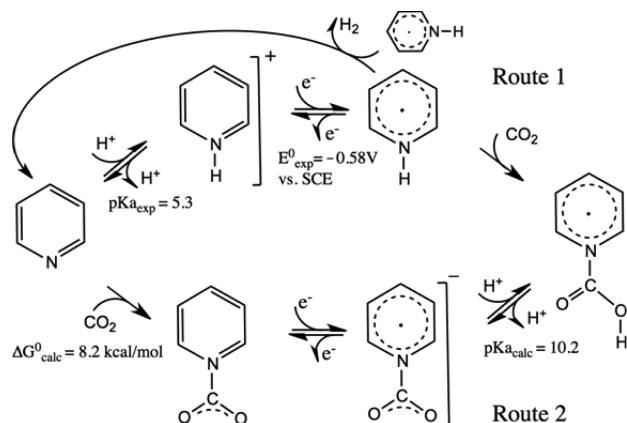
[a]Route 1 involves protonation of Py to PyH[+], reduction of PyH[+] to PyH[0], and finally reduction of CO_2 by PyH[0] to form PyCOOH[0]. Route 2 involves complexation of Py and CO_2, reduction of Py·CO_2, and finally protonation of PyCOO[−] to PyCOOH[0].

CH_3OH through a series of subsequent reduction steps. Route 2 is an alternative path that first involves the formation of the zwitterionic complex Py·CO_2, which is then reduced and subsequently protonated. Bocarsly et al. determined that Route 2 does not contribute significantly to the overall reduction of CO_2 due to the presence of Py·CO_2 at low concentration,[40] consistent with our calculated equilibrium constant of 1.0×10^{-6} for Py·CO_2 formation (see SI, section 2).

In contrast, experimental evidence suggests that PyCOOH[0] formation proceeds through Route 1. The pK_a of Py is 5.3, and thus at a pH of 5.2 (slight acidic conditions due to the acid dissociation equilibrium of CO_2/Py species in aqueous solution) ~40% of Py is protonated in aqueous solution at equilibrium. Consequently, a considerable concentration of PyH[+] exists in the bulk solution, which can then be reduced to form PyH[0] either electrochemically[40,42,45] at various metal electrodes with different values of E^0 (see above) or photoelectrochemically by photoexcited p-GaP.[40] The reported −0.58 V (vs SCE) E^0 of PyH[+] was measured on a Pt surface, whereas E^0 at p-GaP is unknown. The PyH[0] formed by this reduction can then operate as an active species that is proposed to react with CO_2 to form PyCOOH[0] through inner-sphere ET.[40] Alternatively, as shown in Scheme 1, two PyH[0]'s can form H_2 as an unwanted side reaction[40,42] through a self-quenching reaction at a rate constant of ~10^8 M^{−1} s^{−1}.[52] However, the concentration of PyH[0] derived from Bocarsly et al.'s reported CV is only ~10^{-9} M.[40] At this low concentration, the bimolecular self-quenching rate is estimated to be only ~10^{-10} M s^{−1}, consistent with the observed nearly reversible CV. In contrast, the concentration of CO_2 in the solution is ~30 mM, more than ~10^7 times that of PyH[0]. Therefore, the bimolecular collision probability between PyH[0] and CO_2 is much higher than for PyH[0] self-quenching.

While the PyH[0] radical has been proposed as the active species catalyzing CO_2 reduction in this system, here we present a detailed mechanism with associated energetics for PyCOOH[0] formation from PyH[0] and CO_2 including kinetic barriers and TS structures and a specific description of Py's mechanism of activation. We calculate a high pK_a for PyH[0] of ~31, in agreement with Keith et al.'s calculated pK_a of ~27,[43] indicating that deprotonation of PyH[0] is thermodynamically

unfavorable. Furthermore, Bocarsly et al. proposed that interaction between PyH[0] and the p-GaP surface may facilitate deprotonation or dissociation of the N−H bond of PyH[0].[41] Our results do not rule out active participation of p-GaP in activating PyCOOH[0] formation.[53] However, we do predict a pathway for homogeneous PyCOOH[0] formation with kinetics consistent with experiment[41] where the p-GaP[39] or other metal surfaces[40,42,45] only serve as the donor of a high-energy electron with sufficient energy to reduce PyH[+]. We also show that the effects of proton shuttling and aromatic stabilization play key roles in the overall PCET process, catalyzing N−H bond dissociation and PyCOOH[0] formation, which have not been previously proposed.

The goals of this paper are: (i) to identify a mechanism for homogeneous CO_2 reduction in this system, (ii) to determine whether this mechanism is kinetically viable, (iii) to elucidate the role of aqueous solvent in catalyzing PyCOOH[0] formation through prediction of the activation barriers of possible pathways, (iv) to identify the properties of PyH[+]/PyH[0] that enable it to perform as a 1e[−] transfer mediator to facilitate CO_2 reduction, and (v) to uncover the principles of CO_2 reduction at work in this system. We anticipate that the understanding our results provide will guide the catalyst community to discover additional systems similar to PyH[0] competent in reducing CO_2.

2. COMPUTATIONAL DETAILS

The results we report were calculated using the unrestricted coupled-cluster method uCCSD(T)[54] combined with the cc-PVDZ, cc-PVTZ,[55,56] and 6-311++G**[57] basis sets and the Restricted-Open Shell Moller−Plesset second-order perturbation method[58] (roMP2) combined with the 6-31+G** basis set as implemented in the GAMESS[59,60] and Gaussian09[61] computational chemistry software packages. Computational details of the calculated adsorption energies discussed in the Introduction are provided in the SI, section 1. roMP2 was chosen over the unrestricted uMP2 method largely because of its higher computational efficiency. The use of roMP2 was validated using both uCCSD(T) and uMP2 where roMP2/6-31+G** reproduces uCCSD(T)/cc-PVDZ enthalpic barriers evaluated at roMP2/6-31+G** geometries to within ~1.0 kcal/mol and uMP2/6-31+G** enthalpic barriers to within 2.5 kcal/mol (see Table 1). At the uCCSD(T) level of theory, the cc-PVDZ, cc-PVTZ, and 6-311++G** basis sets result in similar enthalpic barriers (within ~2.5 kcal/mol) for PyH[0] + CO_2 (see footnote of Table 1).

We determined that the open-shell systems investigated are doublets and are not significantly multireference. Thus, they are well represented using a single Slater determinant by examining all stationary structures along the PyH[0] + CO_2 + $1H_2O$ (where a single H_2O acts as a proton relay) reaction pathway at the complete active space CASSCF (15,14) level of theory.[62] We found each structure to be dominantly composed (greater than 0.9 coefficient) of the ground state electronic configuration (see SI, section 3). Thus, the high-level uCCSD(T) method should provide a reliable benchmark for energies for this reaction (see Table 1). We found that various density functional theory (DFT) methods produced results with artifacts associated with DFT's tendency to over stabilize zwitterionic charge transfer states, which arises from self-interaction and delocalization errors.[63−66] This is problematic when describing processes involving ET and aromaticity such as the PCET process catalyzed by PyH[0] examined here.

All reactant and product structures were verified to have real vibrational frequencies; meanwhile, TSs were verified to have only one imaginary frequency corresponding to the reaction coordinate of interest as confirmed by both inspection of the normal mode and intrinsic reaction coordinate (IRC) calculations. Frequency calculations at the roMP2/6-31+G** level of theory were also employed for

Table 1. Enthalpic Barriers and Reaction Enthalpies for the Reaction of $PyH^0 + CO_2 + mH_2O + nH_2O(S)$ To Form $PyCOOH^0$, Where m is the Number of Active H_2O's in the Proton Relay and n is the Number of Solvating H_2O's

system[a]	ΔH^0_{act}		ΔH^0_{rxn}	
	$CCSD(T)^b$	$MP2^c$	$CCSD(T)^b$	$MP2^c$
(a) $PyH^0 + CO_2$	46.8^d	45.7	9.3^e	8.9^e
(b) $PyH^0 + CO_2 + H_2O$	29.9	29.5^f	5.7^e	6.0^e
(c) $PyH^0 + CO_2 + 2H_2O$	21.2	20.4	3.4^e	3.3^e
(d) $PyH^0 + CO_2 + 3H_2O$	18.6	18.5	−5.2	−3.2
(e) $PyH^0 + CO_2 + 3H_2O + H_2O(S)$	–	16.5	–	−2.2
(f) $PyH^0 + CO_2 + 3H_2O + 4H_2O(S)$	–	14.6	–	−4.0
(g) $PyH^0 + CO_2 + 2H_2O + 5H_2O(S)$	–	14.6	–	$0.6^{e,g}$
(h) $PyH^0 + CO_2 + 3H_2O + 6H_2O(S)$	–	14.5^h	–	−4.2
(i) $PyH^0 + CO_2 + 3H_2O + 10H_2O(S)$	–	13.6	–	−5.8

^{a}All enthalpies in kcal/mol at 298 K and 1 atm where electrostatic solute−solvent interactions were treated using CPCM with aqueous solvent. In cases e−i, explicit solvent was also employed to treat solvation. ^{b}Single-point uCCSD(T)/cc-PVDZ//roMP2/6-31+G** enthalpies. ^{c}roMP2/6-31+G**. ^{d}Reported barrier at cc-PVDZ (46.8 kcal/mol) basis set agrees with cc-PVTZ (44.5 kcal/mol) and 6-311+ +G** (46.9 kcal/mol). ^{e}Cis isomer of $PyCOOH^0$ was produced (Figure 1c). ^{f}uMP2/6-31+G** produced a similar barrier of 31.9 kcal/mol. $^g PyCOOH^0$ (cis) product with partial PT from H_3O^+ to CO_2 (see SI, section 5). ^{h}15.3 kcal/mol barrier obtained with a different explicit H_2O configuration (see SI section 5).

calculation of zero-point energies (ZPE) and thermal contributions to the enthalpy at 298 K and 1 atm.

All calculations employed the conductor-like polarizable continuum implicit solvent model (CPCM) to describe the effects of solvation,[67,68] where only electrostatic solute−solvent interactions were considered. We used the SMD solvent model[69] to calculate that neglect of nonelectrostatic terms in CPCM leads to errors in the activation enthalpies of less than 2 kcal/mol. The details regarding these SMD calculations and the use of the CPCM model to describe the effects of solvation on enthalpic barriers are described in the SI, section 4. Because CPCM is less accurate in describing solvation of species with concentrated charges,[70−72] we also report energies where explicit H_2O molecules were added to explicitly solvate the system.

In the mechanism of CO_2 reduction catalyzed by PyH^0 we propose that H_2O actively participates in the PCET mechanism by undergoing O−H bond formation and dissociation to transfer protons. Consequently, we explicitly include these active H_2O's as part of the core reaction system. For example, in the $PyH^0 + CO_2 + 3H_2O + 10H_2O(S)$ reaction, three H_2O molecules actively participate in the reaction, while ten H_2O molecules are included to solvate the core reaction system and are labeled as $H_2O(S)$ to indicate that they are *explicit* solvent. For each system, PyH^0 and CO_2 together with the active and solvating water molecules are embedded in a CPCM *implicit* solvent. All explicit H_2O molecules are treated quantum mechanically at the same level of theory as PyH^0 and CO_2. Using explicit solvent introduces challenges associated with particular solvent configurations producing different enthalpic reaction barriers.[73,74] One approach to examine how solvent dynamics leads to kinetic dispersion is to use molecular dynamics to sample the effect of solvent configurations on the reaction barrier.[73] On the other hand, CPCM implicit solvent empirically describes the contributions of solvent configurations to solvation energies in aqueous solutions in close agreement with explicit molecular dynamics.[73] We discuss the effects of solvent configurations on the reaction barrier below and in the SI, section 5.

Atomic charges were calculated using a Mulliken[75] population analysis and the CHELPG electrostatic potential derived charges

method[76] at the roMP2/6-31+G**/CPCM-H2O level of theory. In contrast, adiabatic electron affinity (EA) and E^0 calculations employed the high-level CBS-QB3/CPCM-H2O compound method.[77] E^0's were calculated following the same procedure used by Winget et al. and Tossell;[44,78] details describing this approach can be found in the SI, section 6. pK_a calculations were performed using an approach similar to that used by Liptak et al.,[79] as described in the SI, section 6.

3. RESULTS AND DISCUSSION

High Barrier to Formation of $PyCOOH^0$ for an Unmediated Reaction between PyH^0 and CO_2. The PEC reduction of CO_2 to CH_3OH in the Py/p-GaP system has been observed to proceed at room temperature via a rate-limiting step with an effective activation barrier of 16.5 ± 2.4 kcal/mol.[41] The rate-limiting step for this process has been proposed[41] to be the formation of $PyCOOH^0$ (see Figure 1c
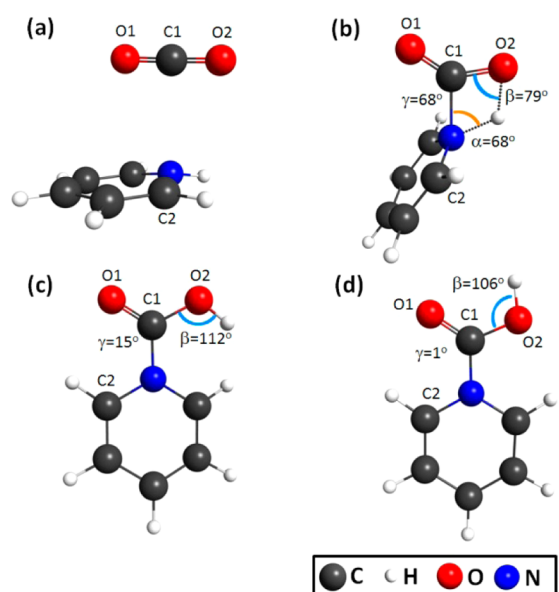

Figure 1. Formation of $PyCOOH^0$ by direct (unmediated) PT from PyH^0 to CO_2. (a) Reactant complex. (b) TS for direct PT; $R_{N−C} = 1.61$ Å, α is the C−N−H angle, and β is the C−O−H angle, as shown. (c) Cis isomer and (d) trans isomer products with γ indicating the dihedral angle O1−C1−N−C2.

and 1d) from PyH^0 and CO_2 where a proton is transferred from the nitrogen atom of PyH^0 to an oxygen atom of CO_2. Figures 1c and 1d show the cis and trans isomers of $PyCOOH^0$ with the trans isomer being the more stable of the two by 6.1 kcal/mol. Our calculations predict a 45.7 kcal/mol enthalpic barrier for this step when it occurs in the homogeneous phase and is modeled as $PyH^0 + CO_2$ in an implicit aqueous solvent. The calculated ~46 kcal/mol barrier lies significantly higher than the experimentally determined barrier of ~17 kcal/mol. Furthermore, we obtained a similar barrier of 46.8 kcal/mol with the high-level uCCSD(T)/roMP2 method, confirming that this pathway is not active at 298 K. Figure 1 shows the optimized reactant, TS, and product structures. In this reaction, the less stable cis isomer of $PyCOOH^0$ (Figure 1c) is formed. We calculate an isomerization barrier of 1.6 kcal/mol to convert the cis isomer to the trans isomer (Figure 1d).

In the formation of $PyCOOH^0$, the reaction proceeds via nucleophilic attack where PyH^0 approaches CO_2 with its N lone pair directed toward the C atom of CO_2. Figure 2 presents a localized orbital representation to illustrate the donation of
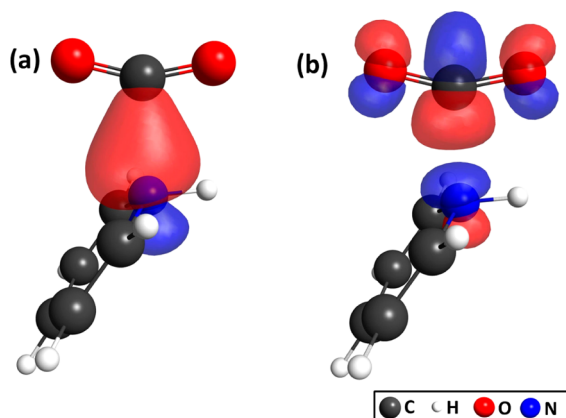
Figure 2. (a) Localized representation of the N lone pair orbital of PyH^0 and (b) localized representation of the π^* orbital of C in CO_2 for a molecular structure along the IRC for $PyCOOH^0$ formation at $R_{N-C} = 2.01$ Å. The TS occurs at $R_{N-C} = 1.61$ Å.

electron density from the PyH^0 N lone pair into the π^* orbital of CO_2 along the reaction coordinate R_{N-C}. As R_{N-C} decreases, CO_2 first bends as a result of nucleophilic attack, and subsequently a proton transfers from PyH^0 to CO_2, suggesting that ET precedes and is coupled to PT (vide infra).

Calculating the energetics of this PCET reaction step does not pose any particularly difficult challenges. For example, proper description of the electronic structure of the reacting system does not require a multireference method and should be well-described by reliable single Slater determinant ab initio methods. Consequently, the considerable disagreement between the barrier for the formation of $PyCOOH^0$ calculated using reliable quantum chemical methods and the experimentally determined barrier suggests that either a heterogeneous process involving the p-GaP electrode catalyzes $PyCOOH^0$ formation[41] or alternative lower barrier pathways occurring in the homogeneous phase may be active. However, a thorough search for alternative TSs for homogeneous formation of $PyCOOH^0$ by direct PT from PyH^0 to CO_2 (TS shown in Figure 1b) yielded no low barrier pathways.

After a comprehensive search did not identify alternative low barrier pathways for the homogeneous formation of $PyCOOH^0$ via direct PT from PyH^0 to CO_2, we hypothesized that H_2O molecules in the aqueous solvent act as proton relays to catalyze $PyCOOH^0$ formation. This supposition was based on thorough inspection of the TS structure for direct PT from PyH^0 to CO_2 (illustrated in Figure 1b), which exhibits considerable strain. The substantial strain present in the TS primarily arises from: (i) bending of the C−O−H angle to 79° relative to its near tetrahedral strain-free angle of 112° in the product structure, (ii) bending of the C−N−H angle to 68° relative to its nearly strain-free angle of between 109° and 120°, and (iii) rotation of the dihedral angle between the Py and CO_2 planes to 68° relative to its angle of 15° in the product. We suggest that H_2O molecules in the aqueous solvent form a *proton shuttling network* that lowers the barrier to $PyCOOH^0$ formation by providing alternative, lower barrier paths for PT from PyH^0 to CO_2. Although PT from PyH^0 to CO_2 via proton shuttling mediated by water is indirect, the TSs involve substantially less strain and thus a considerably lower barrier than direct PT from PyH^0 to CO_2 (vide infra).

Although a proton relay has not been previously proposed for CO_2 reduction in the Py/p-GaP system, proton shuttling

mechanisms have been proposed for a number of other processes.[80−90] While enthalpic barriers to reaction generally determine the kinetics of reactions, especially at low to moderate temperatures, entropic considerations should not be neglected. For example, because CO_2 reduction in the Py/p-GaP system occurs in aqueous solvent, pathways that involve specific solvent configurations may be entropically disfavored. However, if interactions in the solute−solvent system arrange the solvent into configurations that require little solvent reorganization to configure the solvent into the TS structure, a minimal entropic penalty will be required for solvent reorganization to configurations of the TS.

Proton Relay Composed of One to Three Waters. To determine whether a proton relay through water can indeed lower the barrier to $PyCOOH^0$ formation via mediated PT from PyH^0 to CO_2 we calculated the transition states for proton shuttling from PyH^0 to CO_2 through one, two, and three H_2O molecules. In each case, hydrogen bonding positioned the water molecules relative to PyH^0 and CO_2 with the hydrogen atoms of the water arranged to facilitate PT (see Figure 3);
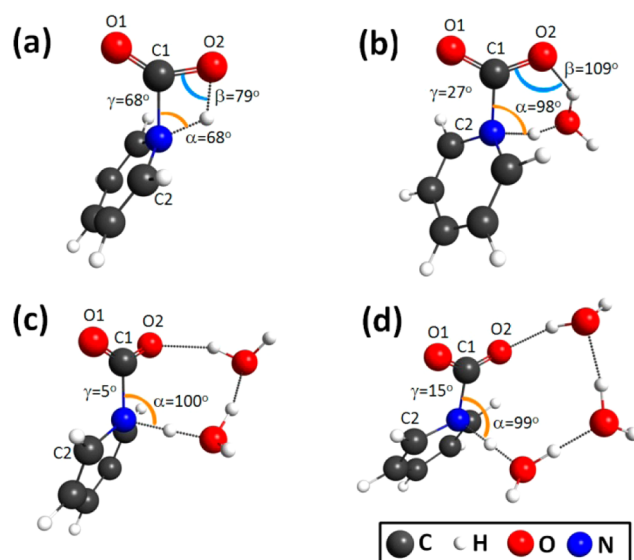

Figure 3. TS structures for the formation of $PyCOOH^0$ via proton shuttling through 0 to 3 H_2O molecules. (a) Direct PT from PyH^0 to CO_2 (same as Figure 1b), (b) PT from PyH^0 to CO_2 mediated by a one water molecule proton relay, (c) PT mediated by a chain of two water molecules, and (d) PT mediated by a chain of three water molecules. α refers to the angle C−N−H and β to the angle C−O−H, and γ refers to the dihedral O1−C1−N−C2.

these configurations are stabilized by significant hydrogen bonding. In addition to the explicit inclusion of water molecules that actively participate in the reaction, the PyH^0 + CO_2 + mH_2O core reaction system (with $m = 1−3$) was solvated in implicit solvent. Figure 3a shows the TS for $PyCOOH^0$ formation via direct PT (repeat of Figure 1b for comparison). Figure 3b shows the TS for $PyCOOH^0$ formation where a single H_2O acts as a proton shuttle between PyH^0 and CO_2; the water molecule concomitantly accepts a proton from the N of PyH^0 and donates a different proton to an O atom of CO_2.

Remarkably, a single water molecule catalyzes $PyCOOH^0$ formation and lowers the barrier 16.2 kcal/mol from $\Delta H^0_{act} = 45.7$ to 29.5 kcal/mol. The TS for $PyCOOH^0$ formation via proton shuttling through one H_2O molecule involves little strain: (i) the C−O−H angle (β) in the TS is 109°, similar to

its angle of 112° in the product; (ii) the C−N−H angle (α) in the TS is 98°, close to the strain-free angle between 109° and 120°; and (iii) the dihedral angle (γ) between the Py and CO_2 planes in the TS is 27°, similar to its angle of 15° in $PyCOOH^0$. Although these results predict that water catalyzes $PyCOOH^0$ formation and facilitates PT from the PyH^0 to CO_2 by shuttling protons, the predicted barrier of 29.5 kcal/mol is still significantly above the experimentally determined barrier of 16.5 kcal/mol for CO_2 reduction in this system. However, this pathway involves only a single water molecule acting as a proton shuttle.

While one water molecule can relay a proton, multiple water molecules can also be arranged to form a chain of proton shuttles where protons are relayed from one water molecule to the next. Figures 3c and d show proton relays composed of a chain of two and three water molecules. When two H_2O molecules are arranged to relay the proton from PyH^0 to CO_2, we calculate that the activation barrier (Figure 3c shows the TS) is lowered to 20.4 kcal/mol. Similarly, arranging three water molecules into a proton-shuttling sequence lowers the barrier to 18.5 kcal/mol (TS shown in Figure 3d). We also examined longer chains of H_2O molecules; however, each relaxed to a chain of three H_2O's with the remaining waters solvating the chain. Like direct PT (Figure 3a), PT from PyH^0 to CO_2 mediated through one and two water molecules produces the higher-energy cis isomer of $PyCOOH^0$, which is easily converted to the more stable trans isomer through a barrier of only 1.6 kcal/mol. In contrast, PT through the three H_2O molecule shuttle yields the more stable $PyCOOH^0$ trans isomer (Figure 1d).

The ability of the three H_2O proton relay to form the more stable $PyCOOH^0$ trans isomer is illustrated in Figure 4. It shows the proton transfer from PyH^0 to CO_2 via a sequence of three H_2O molecules using several structures along the IRC of the reaction step $PyH^0 + CO_2 + 3H_2O \rightarrow PyCOOH^0 + 3H_2O$. The reaction begins at reactant (a), followed by N−C bond formation through nucleophilic attack by the N of PyH^0 on the C of CO_2, similar to the direct PT case presented in Figure 2.
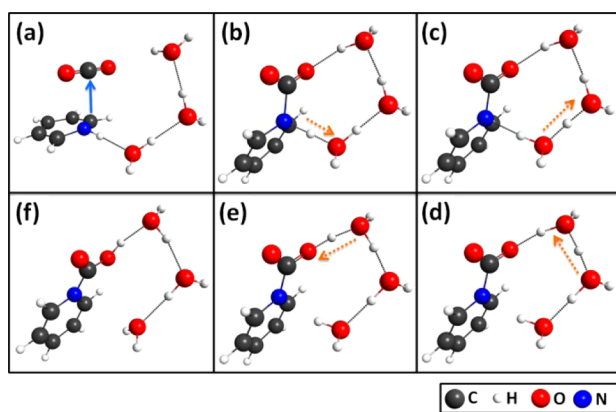

Figure 4. Structures along the IRC for the $PyH^0 + CO_2 + 3H_2O$ reaction step of indirect proton transfer from PyH^0 to CO_2 via a proton relay comprised of a chain of three H_2O molecules. (a) Reactants, (b) TS for $PyCOO^-$ formation by ET followed by PT from PyH^0 to a H_2O, (c) and (d) PT from a H_3O^+ to a neighboring H_2O, (e) PT from H_3O^+ to $PyCOO^-$, and (f) the trans $PyCOOH^0$ product. The dashed orange arrows indicate the direction of PT and the blue arrow the nucleophilic attack on the C of CO_2. A video of this reaction along the IRC is available in the HTML version of the paper.

The reaction then proceeds through (b), a TS for PT from $PyH^0 \cdot CO_2$ to the first water molecule in the shuttling chain, followed by (c) and (d), which show subsequent PTs from H_3O^+ to the next water in the chain, and finally (e), PT from H_3O^+ to $PyCOO^-$ to form (f) $PyCOOH^0$ (trans). The ability of the three H_2O molecule proton relay to produce the more stable trans isomer further demonstrates the ability of the proton shuttle to lower the barrier to form $PyCOOH^0$. We summarize the enthalpic barriers (ΔH^0_{act}) and reaction enthalpies (ΔH^0_{rxn}) at standard conditions in Table 1 for $PyCOOH^0$ formation by various PT pathways involving proton relays formed by different numbers of H_2O molecules. Figure 5 depicts the stationary points along the PES for $PyCOOH^0$ formation from the data in Table 1 and emphasizes proton shuttling in lowering $PyCOOH^0$ formation barriers.
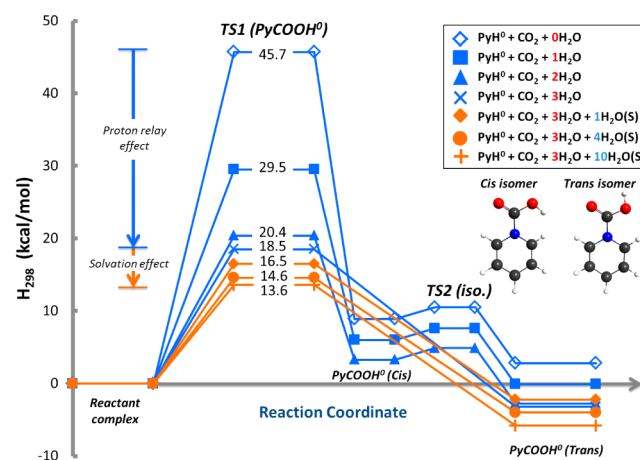

Figure 5. Stationary points along the potential energy surfaces for $PyCOOH^0$ formation via both direct and indirect (via the water proton relay) PT from PyH^0 to CO_2. The $PyCOOH^0$ formation barrier (TS1) decreases with increasing number of water molecules m in the proton relay from 0 to 3 and by including explicit water (denoted by S) to solvate the reaction complex. TS2 is for cis−trans isomerization, which lies 1.6 kcal/mol above the cis isomer. Cases g and h reported in Table 1 have been omitted for clarity.

The results shown above demonstrate that the 45.7 kcal/mol barrier to form $PyCOOH^0$ without the aid of the water proton relay is ~30 kcal/mol above the experimentally determined barrier of 16.5 kcal/mol. Furthermore, we predict that the barrier decreases to ~18−20 kcal/mol when multiple water molecules form a proton shuttling relay. As we discuss in detail below, the barrier declines further to between 13.6 and 16.5 kcal/mol when the TSs are calculated with explicit water molecules solvating the reaction complex (Table 1 cases e−i and Figure 5). We speculated that proton shuttling via water may partially lower the reaction barrier by alleviating strain in the TS in the: (i) C−N−H angle, α, (ii) C−O−H angle, β, and (iii) dihedral angle, γ, between the Py and CO_2 planes. Next, we analyze how proton shuttling via water reduces those strains.

Proton Relay Network Reduces Strain in the TS. Figure 1 shows the reactant, TS, and product structures for $PyCOOH^0$ formation for direct PT from PyH^0 to CO_2. While the product has a C−O−H angle of 112°, this angle is 79° in the TS structure. This suggests that part of the activation barrier can be attributed to this angular strain. Although this analysis compares the TS structure to the product rather than the reactant to estimate the strain in the TS from the C−O−H

angle, it still indicates a high-lying TS because this reaction step is relatively thermoneutral (see Table 1). If this reaction was significantly exothermic, this approach to analyzing the strain could be misleading because a reaction with a low barrier in the forward direction could still exhibit a large degree of strain between the TS and product.

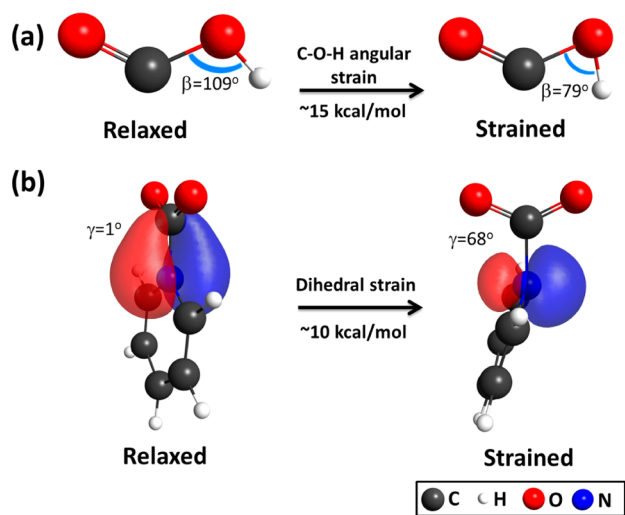We estimate that strain in the C−O−H angle accounts for ~15 kcal/mol of the activation energy (see Figure 6a and the

Figure 6. Strain energy contributions to the activation barrier for PyCOOH^0 formation estimated using (a) COOH^0 as a model to estimate the angular strain in the C−O−H angle, β, and (b) PyCOO$^−$ as a model to estimate the dihedral strain between the Py and CO$_2$ planes, γ.

SI, section 7). In contrast, for the one water molecule proton relay (Figure 3b), the C−O−H angle in the TS is 109°, similar to its angle of 112° in the product, leading to a substantial reduction in strain and a decrease of 16.2 kcal/mol in the barrier (see Table 1). In the cases of the two (Figure 3c) and three (Figure 3d) water molecule proton relays, the TS involves PT to form a H$_3$O$^+$ intermediate. Consequently, the O−H bond of the product is not in the process of forming at the TS. Another potential source of strain is the C−N−H angle. In the event of direct PT (Figures 1b or 3a), this angle is 68° compared to a strain-free angle between 109 and 120°; the proton relay partially alleviates this strain, leading to C−N−H angles in the TSs of 98° (one H$_2$O), 100° (two H$_2$O's), and 99° (three H$_2$O's).

Lastly, strain can also be attributed to the rotation of the dihedral angle between the PyH^0 and CO$_2$ planes; i.e., the dihedral angle is 68° at the TS versus 15° in the product PyCOOH^0. Using PyCOO$^−$ as a model system, we determined that this dihedral strain contributes ~10 kcal/mol to the activation barrier (see Figure 6b), which is consistent with the 16 kcal/mol barrier to internal rotation of this dihedral previously calculated by Han et al.[91] They explained that the barrier to rotation of this dihedral angle arises from the π character of the N−C bond,[91] which is supported by the N−C π orbital shown in Figure 6b.

Adding Solvating Waters to the PyH^0 + CO$_2$ + 3H$_2$O System. Although CPCM generally calculates solute–solvent electrostatic interactions correctly, it describes solvation of solutes possessing concentrated charges less accurately.[70−72] For example, the negative charge of the PyCOO$^−$ complex at

the TS is concentrated on CO$_2$ (discussed further below), and consequently, CPCM may not accurately describe solvation of this TS. Thus, to determine the effect of describing the solvation of species with concentrated charge, we also employed explicit H$_2$O to solvate the reacting system.[74,92] To examine the significance of including explicit solvent, we added one, four, six, and ten additional H$_2$O molecules to solvate the reaction core consisting of PyH^0, CO$_2$, and the H$_2$O's of the proton relay. These additional water molecules were treated at the same level of theory as the rest of the system. Similar to the previously discussed calculations, the PyH^0 + CO$_2$ + 3H$_2$O + nH$_2$O(S) systems, consisting of the core reactive system and n explicit solvating water molecules, are embedded in a continuum polarizable solvent. The effect of additional explicit solvent is reflected in the results shown in Table 1, entries e−i, and Figure 5. We find that adding one solvating water molecule to hydrogen bond with an O of CO$_2$ and a H of the neighboring H$_2$O of the proton relay included in the PyH^0 + CO$_2$ + 3H$_2$O core reaction system (Figure 7a) decreases the
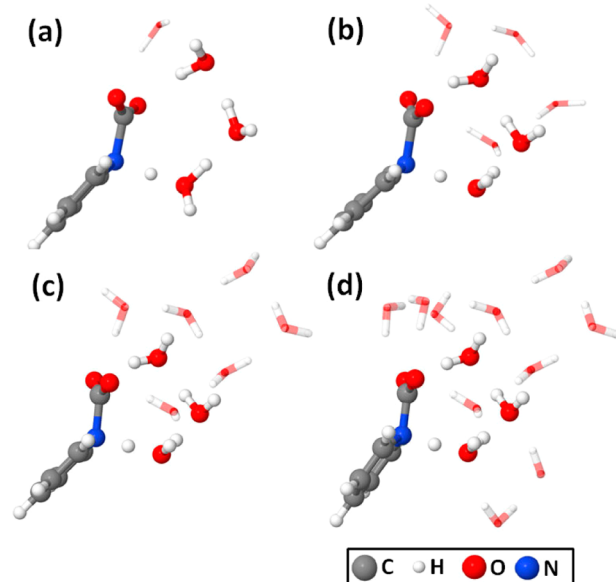

Figure 7. TS structures for PyCOOH^0 formation via a proton shuttling network formed by three H$_2$O molecules (illustrated using a ball-and-stick model) and (a) one, (b) four, (c) six, and (d) ten solvating H$_2$O's. Solvating H$_2$O's are depicted by a stick model.

barrier by 2 kcal/mol, to 16.5 kcal/mol. Adding four and six solvating H$_2$O's (Figure 7b and c) only decreases the barrier by 4 kcal/mol to 14.6 and 14.5 kcal/mol. Finally, upon adding ten solvating H$_2$O's, the reaction barrier decreases to 13.6 kcal/mol, as shown in Figure 7d. In the SI, section 5, we show that the barrier calculated using four to ten explicit solvating H$_2$O's is converged within the accuracy of the methods employed.

Adding multiple solvating H$_2$O molecules leads to stabilization of one of the shuttling protons such that a H$_3$O$^+$ intermediate results. Here, the 14.6, 14.5, and 13.6 kcal/mol barriers for four, six, and ten solvating H$_2$O's, respectively, are the activation energies to form the PyCOO$^−$ (PyCOO$^−$·H$_3$O$^+$·2H$_2$O) intermediate rather than PyCOOH^0. In these three cases, the formation of PyCOOH^0 proceeds through a second TS where a proton is relayed from the H$_3$O$^+$·2H$_2$O complex to PyCOO$^−$ with a negligible activation energy (less than 0.1 kcal/mol at 0 K) which becomes

barrierless upon addition of the ZPE and the thermal correction at 298 K. Thus, the 14.6, 14.5, and 13.6 kcal/mol barriers to form the $PyCOO^- \cdot H_3O^+$ intermediate are effectively the barriers to form $PyCOOH^0$, and this pathway contributes to the overall rate of $PyCOOH^0$ formation. We calculated a pK_a of 10.2 for $PyCOO^-/PyCOOH^0$, thus $PyCOOH^0$ should dominate over $PyCOO^-$ at thermodynamic equilibrium. Our results demonstrate that inclusion of explicit H_2O molecules to solvate the active reaction complex lowers the reaction barrier. This effect is caused by additional solvent stabilization of the concentrated charges on CO_2 (in the $PyCOO^-$ complex) at the TS relative to the reactants compared to what is provided by the implicit CPCM solvent. However, the lowering of the activation barrier from 18.5 kcal/mol (CPCM only) to 13.6 kcal/mol (ten $H_2O(S)$ case) is likely overestimated.

Inclusion of an explicit first solvation shell with no surrounding solvent can result in overpolarization between the explicit solvent and the core reaction system[73] due to the absence of interactions with additional solvation shells. In the case of aqueous solvent and a TS more polar than the reactants, this may result in excessive lowering of the activation barrier. However, embedding of the explicit solvent in implicit solvent mitigates this effect through interactions of the infinite bath of implicit solvent with the first solvation shell. For example, the PCET barrier for $PyH^0 + CO_2 + 3H_2O + 4H_2O(S)$ increased from 12.5 kcal/mol (gas phase) to 14.6 kcal/mol (CPCM) with addition of implicit solvent (see the SI, section 4). The extent to which CPCM alleviates the error of overpolarization of the first solvation shell effect is unknown and beyond the scope of this study. However, for $PyH^0 + CO_2 + 3H_2O$, the results with explicit solvent (overpolarization) and CPCM only (under-polarization), respectively, set a lower and an upper bound to the barrier; thus, our results predict that the PCET barrier lies between 13.6 and 18.5 kcal/mol.

Introduction of explicit solvent can introduce additional challenges due to the large solvent configurational space. For example, particular solvent configurations stabilize the TS relative to the reactants more than others. These configurational variations introduce a distribution of enthalpic barriers.[73] For example, in Table 1, we report the barrier for $PyH^0 + CO_2 + 3H_2O + 6H_2O(S)$ to be 14.6 and 15.3 kcal/mol in two possible solvent configurations (see SI, section 5). Solvent reorganization due to thermal fluctuations introduces similar effects and consequently a distribution of enthalpic barriers such that the experimentally determined barrier corresponds to an ensemble average over many solvent configurations. The barriers involving explicit H_2O reported in Table 1 are calculated for only a few of the many possible configurations that can contribute to the ensemble averaged barrier. Moreover, configurations that result in proton relays composed of various numbers of H_2O can contribute to the ensemble averaged barrier. For instance, the barrier for $PyH^0 + CO_2 + 2H_2O + 5H_2O(S)$ in a two water proton relay is 14.6 kcal/mol (Table 1, entry g), similar to the barrier of the three water proton relay.

Comparison with the Experimentally Determined Barrier. Our results demonstrate the central role of proton shuttling via water in catalyzing the formation of $PyCOOH^0$, where shuttling through the three water molecule relay lowers the reaction barrier by ~27 kcal/mol relative to direct PT. The 18.5 kcal/mol barrier for $PyH^0 + CO_2 + 3H_2O$ modeled in CPCM, confirmed by high-level CCSD(T) results, should provide a reliable baseline estimate for the activation barrier to form $PyCOOH^0$ from the reaction of PyH^0 and CO_2 in the

homogeneous phase because the continuum description of the solvent implicitly averages out the variations in the enthalpic barrier resulting from solvent fluctuations despite its limitation in describing solute with concentrated charges.[73,93] To better describe interaction between the solvent and the solute with localized charges, four, six, and ten solvating H_2O's were included. These models all predicted a barrier within 0.5 kcal/mol of 14.1 kcal/mol, which is well within the accuracy of roMP2. Thus, 14.1 ± 0.5 kcal/mol provides our best estimate of the barrier for the three water proton relay configuration, assuming that CPCM alleviates most of the overpolarization of the TS by the first solvation shell (see discussion above). This estimate does not explicitly consider how other solvent configurations might affect the barrier beyond demonstrating that it changes by less than 1 kcal/mol for four to ten explicit H_2O's and for two different solvent configurations for the case of six explicit solvating H_2O's, as shown in Table 1. Moreover, the two water proton relay also proves to be a viable pathway with a 14.6 kcal/mol barrier for $PyH^0 + CO_2 + 2H_2O + 5H_2O(S)$ (see Table 1, case g).

We propose that the experimentally determined barrier of 16.5 ± 2.4 kcal/mol is consistent with a weighted average of active pathways that consist of proton transfers through relays of one to three H_2O molecules where the ensemble-averaged barrier depends on both the configurational and Boltzmann weight for each pathway. Although an exhaustive examination of all possible pathways and calculation of the configurational weights for the pathways we report is beyond the scope of this study, the ensemble average for the lowest-energy pathways we report must lie within the range of 13.6 kcal/mol (two and three water proton relays) and 22.8 kcal/mol (one water proton relay, see SI, section 5 for estimation of this barrier). Because the barrier for reaction through the one H_2O shuttle is ~9 kcal/mol larger than the barrier for PCET through two and three H_2O's, the configurational weight on the one H_2O shuttle must be at least ~10^6 times larger for it to contribute significantly to the reaction rate at 298 K. For example, with relative configurational weights of 10^5 and 10^6 on the one H_2O shuttle pathway and configurational weights of one on each of the two and three H_2O shuttle pathways, the average barriers are 13.9 and 14.9 kcal/mol, respectively. Consequently, although it is possible that other active pathways exist and we do not explicitly calculate the configurational weights required for evaluating the ensemble-averaged barrier, we expect that ensemble averaging the pathways we report will result in a predicted barrier of between 13.6 and 15 kcal/mol.

These results predict that the homogeneous formation of $PyCOOH^0$ is viable, mediated by proton shuttling in aqueous solvent, and does not require the p-GaP electrode surface to play an active role in N–H bond cleavage of PyH^0. However, it is also possible that the experimentally measured barrier corresponds to thermally activated desorption of PyH^0 from the Pt electrode to the homogeneous phase. In the Py/Pt system, the measured reduction potential for PyH^+ suggests that desorption of PyH^0 from Pt into the homogeneous phase requires at least 16.8 kcal/mol (see Introduction), a value that coincides with both the experimentally determined barrier and our calculated barrier for homogeneous reaction between PyH^0 and CO_2. Consequently, desorption of the reduced PyH^0 species from Pt may limit $PyCOOH^0$ formation. However, the observed first-order dependence on both PyH^+ concentration and CO_2 concentration is indicative of a bimolecular homogeneous process.[41] We suggest that use of an electrode

material with minimal surface effects on the reduction of PyH^+ (e.g., a Pb or dropping Hg electrode) should exhibit the homogeneous barrier for catalytic reduction of CO_2 by PyH^0. However, aqueous solvent should be used with caution because the homogeneous E^0 of PyH^+ (−1.31 V vs SCE) is more negative than the reduction potential of H_2O, E^0 = −1.07 V vs SCE.

Charge Analysis, pK_a, and EA All Show Stepwise ET Followed by PT. Next, we examine the interplay between ET and PT from PyH^0 to CO_2 to accomplish the chemical reduction of CO_2 through the formation of $PyCOOH^0$. Fundamental questions at the heart of pyridine-catalyzed reduction of CO_2 include: Do ET and PT occur concomitantly or sequentially? If sequentially, in what order do ET and PT occur? In this section, we focus on providing insight into these questions to understand the nature of CO_2 reduction in this system to reveal the role of the Py catalyst in CO_2 reduction. Figure 8 shows a plot of the net charges on PyH^0 and CO_2 as a
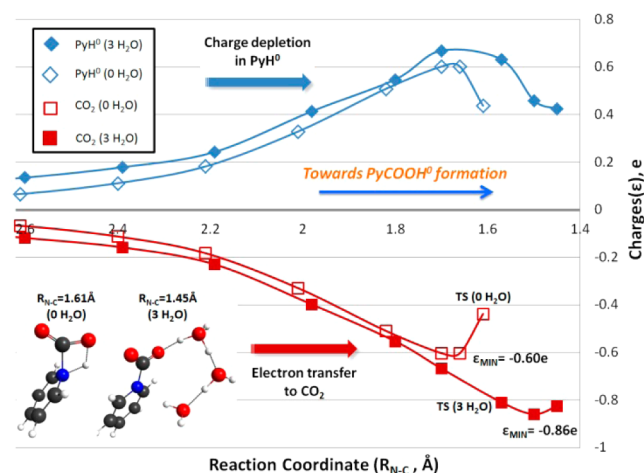

Figure 8. Charges on PyH^0 (blue) and CO_2 (red) along the IRC for $PyCOOH^0$ formation from PyH^0 and CO_2. (0 H_2O) and (3 H_2O) denote the cases of no proton relay (direct PT) and a three H_2O molecule proton relay. ET from PyH^0 to CO_2 is significant at N−C distances significantly longer than the TS (~1.6 Å). Charges determined using the CHELPG method at roMP2/6-31+G**.

function of the distance between the N of PyH^0 and the C of CO_2, which we define as R_{N-C}. The atomic charges were determined using the CHELPG method for several structures along the IRC of $PyCOOH^0$ product formation to delineate the details of the ET process. A charge analysis based on Mulliken populations shows the same qualitative trend as CHELPG-derived atomic charges (see SI, section 8).

In particular, we examine the net charges on CO_2 and PyH^0 for two cases: $PyCOOH^0$ formation in the absence of the proton shuttling network (direct PT) and $PyCOOH^0$ formation mediated by proton shuttling through three water molecules. For both cases, the charge on CO_2 becomes negative, while the charge on PyH^0 becomes more positive as the reaction proceeds from reactant toward the TS along the IRC (see Figure 8). This result demonstrates that ET from PyH^0 to CO_2 occurs as the N−C bond is formed and prior to PT. The charge transfer involves the donation of the N lone pair into a π^* orbital of CO_2, as shown in Figure 2. For the case of no proton shuttle, the charge on CO_2 reaches a minimum of −0.60 e at R_{N-C} = 1.66 Å and increases to −0.44 e at the TS (R_{N-C} = 1.61 Å) because the proton is now partially transferred

to CO_2 along with its partial positive charge (see inset of Figure 8). These results predict that reduction of CO_2 through $PyCOOH^0$ formation occurs through a stepwise charge transfer mechanism where ET to reduce CO_2 precedes PT. Our calculations predict this same mechanism for the case of $PyCOOH^0$ formation through the three H_2O molecule proton relay. In this case, the charge decreases to a minimum of −0.86 e at R_{N-C} = 1.50 Å, just after the TS at R_{N-C} = 1.57 Å, followed by the onset of PT to CO_2 at R_{N-C} = 1.45 Å (see inset of Figure 8 for the structure at R_{N-C} = 1.45 Å).

An alternative mechanism might occur by PyH^0 first transferring its proton to CO_2, followed by ET to reduce CO_2. However, we calculate a pK_a of 31 for PyH^0 in agreement with Keith et al.'s calculated pK_a of ~27.[43] This suggests that direct PT from PyH^0 to CO_2 without ET first is highly thermodynamically unfavorable because it leads to the formation of the high-energy Py^- anionic radical. The energetic cost to form the Py^- anionic radical, either by direct PT from PyH^0 or ET to Py, is also evident from the adiabatic electron affinity (EA) analysis summarized in Table 2, which also lists

Table 2. Adiabatic Electron Affinities (EAs) and Homogeneous Standard Reduction Potentials (E^0 vs SCE)

system[a]	EA[b]	E^{0c}
(a) $Py + CO_2 + e^- = Py^- + CO_2$	37.9	−2.90
(b) $Py + CO_2 + e^- = Py + CO_2^-$	47.4	−2.34, exp. −2.18[51]
(c) $Py + CO_2 + e^- = PyCOO^-$	66.3	−2.05
(d) $PyH^+ + e^- = PyH^0$	73.9	−1.31

[a]Calculations performed using CBS-QB3/CPCM-H_2O. [b]EA = $-\Delta H^0_{reduction}$ in aqueous solution in kcal/mol. [c]E^0 in aqueous solvent in V vs SCE.

our calculated E^0 values for related Py and CO_2 species. We find that Py^- formation is even less favorable than formation of the high-energy CO_2^- anionic radical as demonstrated by our calculations showing that Py's EA of 37.9 kcal/mol is less positive than CO_2's EA of 47.4 kcal/mol. These calculated EAs are consistent with Tossell's CBS-QB3 thermochemical calculations for a number of reduced Py complexes.[44] This analysis based on the pK_a of PyH^0 and the EA's of CO_2 and PyH^0 clearly demonstrates that if PyH^0 and CO_2 were to react ET must precede PT to avoid the high-energy cost of producing the Py^- anionic radical. This result explains and confirms the results of the charge analysis described above.

Formation of the $PyCOO^-$ Anionic Complex Provides a Low-Energy Pathway for ET. The calculated high pK_a of PyH^0, low EA of Py, and net charge versus IRC analysis all suggest that ET to CO_2 must precede PT in the formation of $PyCOOH^0$. If this is indeed the case, what then enables ET, especially given the fact that the anionic radical CO_2^- is high energy? The answer lies in the unusual nature of the $PyCOO^-$ complex (Figure 6b, left), and it is this anionic complex that forms, not CO_2^-. As shown in Figure 9 and Table 2, the $PyCOO^-$ anionic complex is significantly more stable than the CO_2^- or Py^- anions as reflected by their EAs, consistent with Tossell's calculations.[44] It is this unusual stability of $PyCOO^-$ that provides a low-energy pathway for ET from PyH^0 to CO_2 and which results in forming $PyCOO^-$. Formation of the $PyCOO^-$ anionic complex in the three H_2O proton shuttle case is evident in Figure 4c−e, where $PyCOO^-$ is formed transiently after ET and during PT by proton shuttling through the three water molecule chain en route to $PyCOOH^0$ formation. Thus,
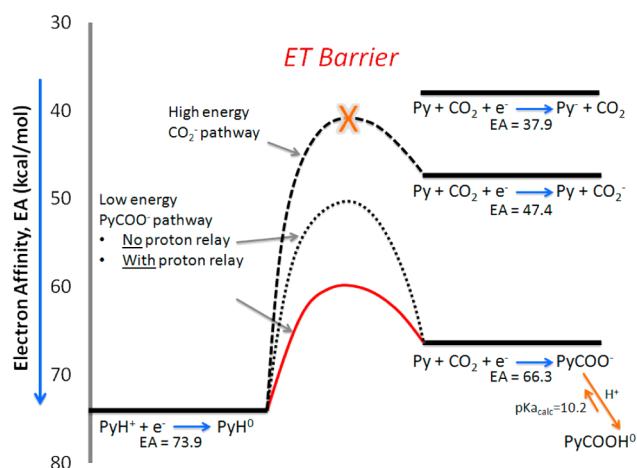
Figure 9. Formation of the PyCOO$^-$ anionic complex mediated by the proton relay provides a low-energy pathway for ET en route to formation of the PyCOOH^0 carbamate species. The ET barriers are shown schematically.

Figure 10. Stabilization of the PyCOO$^-$ complex through aromatic resonance stabilization. PyH^0 possesses seven electrons in its π system. Nucleophilic attack at the C of CO$_2$ by the N of PyH^0 transfers electron density to CO$_2$ to reduce it while recovering the aromaticity of PyH$^+$ and facilitating proton transfer to form PyCOOH^0.

the formation barriers for PyCOOH^0 shown in Figure 5 and schematically in Figure 9 are primarily the ET energy cost to form PyCOO$^-$ by this low-energy pathway; PyCOO$^-$ is subsequently stabilized by protonation at a calculated pK_a of 10.2. The existence and stability of the PyCOO$^-$ complex is also supported experimentally where Han and Kamrath et al. generated the PyCOO$^-$ complex through high-energy ionization,[91,94] in contrast to the PEC reduction of CO$_2$, where PyCOO$^-$ is generated transiently through homogeneous reaction between PyH^0 and CO$_2$ mediated by the proton relay. These results prompt the question: What provides PyCOO$^-$ with its unusual stability?

Aromatic Resonance Stabilization Stabilizes the PyCOO$^-$ Complex. From the analysis above, we can deduce the role of the pyridine catalyst in the PEC reduction of CO$_2$. Py acts as a catalyst by stabilizing the high-energy anionic radical of CO$_2^-$ by forming the stable PyCOO$^-$ complex, thus providing a low-energy pathway for PyCOOH^0 formation. *What makes PyCOO$^-$ unusually stable? Aromatic resonance stabilization.*[95,96] Reduction of PyH$^+$ to PyH^0 increases the number of π electrons of from six to seven, resulting in a loss of aromaticity and PyH$^+$'s large negative reduction potential (Figure 10). The drive to regain the aromaticity lost upon PyH$^+$ reduction compels ET from PyH^0 to CO$_2$ to transiently form PyCOO$^-$. The resulting negative charge localized on CO$_2$ then drives PT from PyH^0 to CO$_2$ through the water proton relay to ultimately form PyCOOH^0. Six electrons remain in the π system of Py after ET, thus making both PyCOO$^-$ and PyCOOH^0 aromatic and lowering their energy. This stabilizes the TS to lower the PCET barrier, as described by the Evans–Polanyi principle.[97]

Without aromatic stabilization, one electron reduction of CO$_2$ or PT from PyH^0 leading to the one electron reduction of Py to Py$^-$ are both prohibitively high in energy (see Figure 9). We test this suggestion using reduced 1,4-azaborininium radical (AB^0). Because the transferred electron is added to and removed from the sp^2 orbital localized on B, AB^0 maintains its aromaticity on being reduced and during reduction of CO$_2$ via PCET. For reduction of CO$_2$ by PCET from AB^0 we calculate an enthalpic barrier of 33.8 kcal/mol at the MP2 level of theory compared to 18.5 kcal/mol for PyH^0 where three waters act as a proton relay for both cases. The high barrier for AB^0-catalyzed
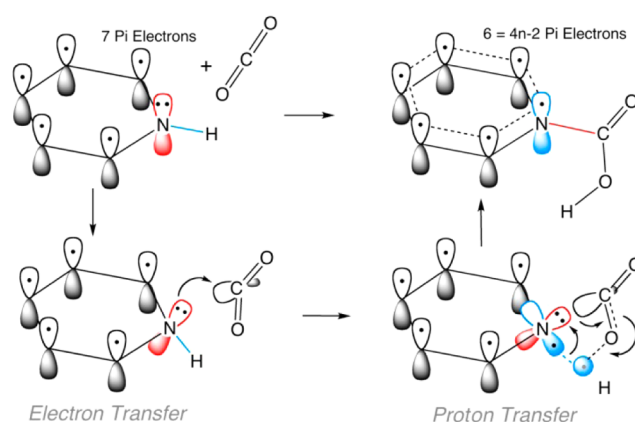
CO$_2$ reduction is a consequence of AB^0 maintaining its aromaticity throughout PCET, thus providing no driving force for ET. Our results provide direct evidence and a detailed and fundamental explanation in support of Bocarsly et al.'s suggestion that Py-catalyzed CO$_2$ reduction proceeds through one electron reduction of CO$_2$.[40] The inverse view in which CO$_2$ stabilizes the high-energy Py$^-$ anionic radical is an equally valid alternative picture of this process. While both views are correct, a more complete analysis demonstrates that Py and CO$_2$ stabilize each other's anionic radical in the form of the PyCOO$^-$ complex.

Proton Shuttling Reduces the Radical Character of the Py Anionic Radical. We emphasize again that ET precedes PT for cases of direct PT and for PT through the H$_2$O molecule relay, as shown in Figure 8. However, the proton relay offers the advantage of more extensive ET to CO$_2$ prior to PT; Figure 8 shows the minimum charge on CO$_2$ for the case of the three H$_2$O molecule relay to be −0.86 e compared to −0.60 e for direct PT in the absence of the relay. The more complete ET to CO$_2$ prior to PT enables Py to approach its low-energy neutral closed-shell state, reducing its high-energy Py$^-$ anionic radical character and consequently lowering the barrier to PyCOOH^0 formation. In other words, we propose that the high 45.7 kcal/mol barrier for direct PT is partially due to the larger Py$^-$ anionic radical character of Py that results from less charge transfer to CO$_2$ prior to PT. Thus, the proton relay provides an additional important effect to catalyze CO$_2$ reduction. In addition to providing a pathway that lowers the strain in the TS, it also provides a favorable configuration that facilitates more complete ET to CO$_2$ during the formation of the PyCOO$^-$ complex to reduce the high-energy anion radical character of Py$^-$ prior to PT. This effect is also consistent with the lowering of the reaction barrier by the proton relay as shown in Figure 5.

Is CO$_2$ Prebent To Facilitate Reduction? The result that ET precedes PT introduces the question of whether CO$_2$ must be prebent to prepare it for reduction where bending CO$_2$ may lower the reorganization energy required for ET. The case where PT is mediated through the three water proton shuttle solvated by ten quantum solvating waters (as shown in Figure 5) exhibits the most extensive ET to CO$_2$ and a barrier of 13.6 kcal/mol for PyCOOH^0 formation. At the TS ET is mostly

complete, and as seen in Figure 7d, CO_2 is not bent prior to ET but is in fact bent as a result of ET. This shows that CO_2 prebending is not a generally required condition to effect low barrier CO_2 reduction.

4. CONCLUSION

We have performed ab initio quantum chemical calculations on proposed pathways for homogeneous $PyCOOH^0$ formation to examine how Py catalyzes the PEC reduction of CO_2 in the Py/p-GaP system. We predict that the barrier to homogeneous $PyCOOH^0$ formation lies between 13.6 and 18.5 kcal/mol where PCET proceeds through a proton relay of three H_2O's and the solvent is modeled using mixed implicit/explicit and only implicit solvation, respectively. A weighted average of PCETs through one to three H_2O relays also falls within this range for weights of the higher barrier one H_2O relay path as large as $\sim10^6$ times the weights on the two and three H_2O relays. Furthermore, this range is consistent with the experimentally determined barrier of 16.5 ± 2.4 kcal/mol. In contrast, in the absence of the proton relay we predict a barrier for direct PT from PyH^0 to CO_2 of ~46 kcal/mol. The predicted solvent-assisted PCET suggests a favorable pathway to CO_2 reduction through $PyCOOH^0$ formation in the homogeneous phase where the purpose of the p-GaP surface is the PEC reduction of PyH^+ to produce active PyH^0 species and may not be an active heterogeneous catalyst for CO_2 reduction. The water proton shuttling network has multiple effects: (a) it reduces the strain in the TS, (b) it produces the more stable $PyCOOH^0$ trans isomer, and (c) it reduces the radical character of the Py^- anion prior to PT. However, it is also possible that the experimentally measured barrier corresponds to endothermic desorption of PyH^0 from the Pt electrode to the homogeneous phase, which requires at least 16.8 kcal/mol of thermal energy, a value that coincides with both the experimentally determined barrier and our calculated barrier for homogeneous reaction between PyH^0 and CO_2.

We determine that Py facilitates the PEC reduction of CO_2 by avoiding the formation of high-energy Py^- and CO_2^- anionic radicals. A population analysis to describe details of charge transfer indicates that $PyCOOH^0$ formation occurs by a stepwise charge transfer mechanism where ET precedes PT. Consequently, the pK_a of PyH^0 is irrelevant in predicting PyH^0's ability to transfer a proton to CO_2. Furthermore, our calculated pK_a of 31 for PyH^0 predicts that PT from PyH^0 does not occur before ET. This is also supported by the calculated EAs of CO_2, Py, and Py·CO_2 which show that the one-electron reductions of CO_2 and Py are prohibitively high in energy, whereas $PyCOO^-$ is a low-energy one-electron reduced state with little radical character. Although the one-electron reduced states of Py and CO_2 are high energy, aromatic resonance stabilization reduces the energies of the transiently formed $PyCOO^-$ anionic complex and $PyCOOH^0$ to lower the barrier to $PyCOOH^0$ formation. We demonstrate that prebending of CO_2 is not a requirement in achieving a low barrier to CO_2 reduction.

ASSOCIATED CONTENT

Ⓢ Supporting Information

PyH^+ adsorption on the Pt surface; K_{eq} calculations for the zwitterionic Py·CO_2 complex; determination of multireference character in the reduction of CO_2 by PyH^0; discussion of CPCM solvation; effects of explicit solvent; E^0 and pK_a calculations; contribution of strain energies to the activation

barrier of $PyH^0 + CO_2$; Mulliken and CHELPG charge analysis; coordinates of molecular structures. This material is available free of charge via the Internet at http://pubs.acs.org.

Ⓦ Web-Enhanced Feature

A video of the proton transfer sequence for the case of the three water proton relay is available in the HTML version of the paper.

■ AUTHOR INFORMATION

Corresponding Author

charles.musgrave@colorado.edu

Notes

The authors declare no competing financial interest.

■ REFERENCES

(1) Beckman, E. J. *Ind. Eng. Chem. Res.* **2003**, *42*, 1598.
(2) Darensbourg, D. J. *Inorg. Chem.* **2010**, *49*, 10765.
(3) Mikkelsen, M.; Jorgensen, M.; Krebs, F. C. *Energy Environ. Sci.* **2010**, *3*, 43.
(4) Choi, S.; Drese, J. H.; Jones, C. W. *ChemSusChem* **2009**, *2*, 796.
(5) Figueroa, J. D.; Fout, T.; Plasynski, S.; McIlvried, H.; Srivastava, R. D. *Int. J. Greenhouse Gas Control* **2008**, *2*, 9.
(6) Jacobson, M. Z. *Energy Environ. Sci.* **2009**, *2*, 148.
(7) Ma, S. Q.; Zhou, H. C. *Chem. Commun.* **2010**, *46*, 44.
(8) White, C. M.; Strazisar, B. R.; Granite, E. J.; Hoffman, J. S.; Pennline, H. W. *J. Air Waste Manage. Assoc.* **2003**, *53*, 645.
(9) Arakawa, H.; Aresta, M.; Armor, J. N.; Barteau, M. A.; Beckman, E. J.; Bell, A. T.; Bercaw, J. E.; Creutz, C.; Dinjus, E.; Dixon, D. A.; Domen, K.; DuBois, D. L.; Eckert, J.; Fujita, E.; Gibson, D. H.; Goddard, W. A.; Goodman, D. W.; Keller, J.; Kubas, G. J.; Kung, H. H.; Lyons, J. E.; Manzer, L. E.; Marks, T. J.; Morokuma, K.; Nicholas, K. M.; Periana, R.; Que, L.; Rostrup-Nielson, J.; Sachtler, W. M. H.; Schmidt, L. D.; Sen, A.; Somorjai, G. A.; Stair, P. C.; Stults, B. R.; Tumas, W. *Chem. Rev.* **2001**, *101*, 953.
(10) Olah, G. A.; Goeppert, A.; Prakash, G. K. S. *J. Org. Chem.* **2009**, *74*, 487.
(11) Olah, G. A.; Prakash, G. K. S.; Goeppert, A. *J. Am. Chem. Soc.* **2011**, *133*, 12881.
(12) Jiang, Z.; Xiao, T.; Kuznetsov, V. L.; Edwards, P. P. *Philos. Trans. R. Soc., A* **2010**, *368*, 3343.
(13) Ganesh, I. *Curr. Sci.* **2011**, *101*, 731.
(14) Hoffmann, M. R.; Moss, J. A.; Baum, M. M. *Dalton Trans.* **2011**, *40*, 5151.
(15) Ashley, A. E.; Thompson, A. L.; O'Hare, D. *Angew. Chem., Int. Ed.* **2009**, *48*, 9839.
(16) Chakraborty, S.; Zhang, J.; Krause, J. A.; Guan, H. *J. Am. Chem. Soc.* **2010**, *132*, 8872.
(17) Cokoja, M.; Bruckmeier, C.; Rieger, B.; Herrmann, W. A.; Kühn, F. E. *Angew. Chem., Int. Ed.* **2011**, *50*, 8510.

(18) Huang, F.; Lu, G.; Zhao, L. L.; Li, H. X.; Wang, Z. X. *J. Am. Chem. Soc.* **2010**, *132*, 12388.

(19) Huang, F.; Zhang, C. G.; Jiang, J. L.; Wang, Z. X.; Guan, H. R. *Inorg. Chem.* **2011**, *50*, 3816.

(20) Menard, G.; Stephan, D. W. *J. Am. Chem. Soc.* **2010**, *132*, 1796.

(21) Zimmerman, P. M.; Zhang, Z. Y.; Musgrave, C. B. *Inorg. Chem.* **2010**, *49*, 8724.

(22) Temkin, O. N.; Zeigarnik, A. V.; Kuz'min, A. E.; Bruk, L. G.; Slivinskii, E. V. *Russ. Chem. Bull.* **2002**, *51*, 1.

(23) Krylov, O. V.; Mamedov, A. K. *Usp. Khimii.* **1995**, *64*, 935.

(24) Dai, W. L.; Luo, S. L.; Yin, S. F.; Au, C. T. *Appl. Catal., A* **2009**, *366*, 2.

(25) Benson, E. E.; Kubiak, C. P.; Sathrum, A. J.; Smieja, J. M. *Chem. Soc. Rev.* **2009**, *38*, 89.

(26) Rakowski Dubois, M.; Dubois, D. L. *Acc. Chem. Res.* **2009**, *42*, 1974.

(27) Savéant, J.-M. *Chem. Rev.* **2008**, *108*, 2348.

(28) Agarwal, J.; Johnson, R. P.; Li, G. *J. Phys. Chem. A* **2011**, *115*, 2877.

(29) Alstrum-Acevedo, J. H.; Brennaman, M. K.; Meyer, T. J. *Inorg. Chem.* **2005**, *44*, 6802.

(30) Huang, K.-W.; Han, J. H.; Musgrave, C. B.; Fujita, E. *Organometallics* **2006**, *26*, 508.

(31) Meyer, T. J. *Acc. Chem. Res.* **1989**, *22*, 163.

(32) Aurian-Blajeni, B.; Halmann, M.; Manassen, J. *Sol. Energy* **1980**, *25*, 165.

(33) Halmann, M. *Nature* **1978**, *275*, 115.

(34) Kumar, B.; Llorente, M.; Froehlich, J.; Dang, T.; Sathrum, A.; Kubiak, C. P. *Annu. Rev. Phys. Chem.* **2012**, *63*, 541.

(35) Morris, A. J.; Meyer, G. J.; Fujita, E. *Acc. Chem. Res.* **2009**, *42*, 1983.

(36) Tran, P. D.; Wong, L. H.; Barber, J.; Loo, J. S. C. *Energy Environ. Sci.* **2012**, *5*, 5902.

(37) Yotsuhashi, S.; Deguchi, M.; Zenitani, Y.; Hinogami, R.; Hashiba, H.; Yamada, Y.; Ohkawa, K. *Applied Physics Express* **2011**, *4*.

(38) Yui, T.; Kan, A.; Saitoh, C.; Koike, K.; Ibusuki, T.; Ishitani, O. *ACS Appl. Mater. Interfaces* **2011**, *3*, 2594.

(39) Barton, E. E.; Rampulla, D. M.; Bocarsly, A. B. *J. Am. Chem. Soc.* **2008**, *130*, 6342.

(40) Cole, E. B.; Lakkaraju, P. S.; Rampulla, D. M.; Morris, A. J.; Abelev, E.; Bocarsly, A. B. *J. Am. Chem. Soc.* **2010**, *132*, 11539.

(41) Morris, A. J.; McGibbon, R. T.; Bocarsly, A. B. *ChemSusChem* **2011**, *4*, 191.

(42) Seshadri, G.; Lin, C.; Bocarsly, A. B. *J. Electroanal. Chem.* **1994**, *372*, 145.

(43) Keith, J. A.; Carter, E. A. *J. Am. Chem. Soc.* **2012**, *134*, 7580.

(44) Tossell, J. A. *Comput. Theor. Chem.* **2011**, *977*, 123.

(45) Yasukouchi, K.; Taniguchi, I.; Yamaguchi, H.; Shiraishi, M. *J. Electroanal. Chem. Interfacial Electrochem.* **1979**, *105*, 403.

(46) Hickey, J. E.; Spritzer, M. S.; Elving, P. J. *Anal. Chim. Acta* **1966**, *35*, 277.

(47) Tompkins, P. C.; Schmidt, C. L. A. *J. Biol. Chem.* **1942**, *143*, 643.

(48) Shikata, M.; Tachi, I. *J. Agric. Chem. Soc. Jpn.* **1927**, *3*, 746.

(49) Jenkins, S. J. *Proc. R. Soc. A* **2009**, *465*, 2949.

(50) Bard, A. J.; Faulkner, L. R. *Electrochemical Methods: Fundamentals and Applications*, 2nd ed.; Wiley: New York, 2001.

(51) Koppenol, W. H.; Rush, J. D. *J. Phys. Chem.* **1987**, *91*, 4429.

(52) Leuschner, R.; Krohn, H.; Dohrmann, J. K. *Ber. Bunsen-Ges. Phys. Chem. Chem. Phys.* **1984**, *88*, 462.

(53) Muñoz-García, A. B.; Carter, E. A. *J. Am. Chem. Soc.* **2012**, *134*, 13600.

(54) *Coupled-cluster theory*; J. Paldus, i. S. W. a. G. H. F. D., Ed.; Plenum: New York, 1992; Vol. 293.

(55) Woon, D. E.; Dunning, T. H. *J. Chem. Phys.* **1993**, *98*, 1358.

(56) Dunning, T. H. *J. Chem. Phys.* **1989**, *90*, 1007.

(57) Harihara, Pc; Pople, J. A. *Theor. Chim. Acta* **1973**, *28*, 213.

(58) Binkley, J. S.; Pople, J. A. *Int. J. Quantum Chem.* **1975**, *9*, 229.

(59) Schmidt, M. W.; Baldridge, K. K.; Boatz, J. A.; Elbert, S. T.; Gordon, M. S.; Jensen, J. H.; Koseki, S.; Matsunaga, N.; Nguyen, K. A.; Su, S. J.; Windus, T. L.; Dupuis, M.; Montgomery, J. A. *J. Comput. Chem.* **1993**, *14*, 1347.

(60) Gordon, M. S.; Schmidt, M. W. In *Theory and Applications of Computational Chemistry*; Clifford, E. D., Gernot, F., Kwang, S. K., Dykstra, C. E., Frenking, G., Kim, K. S., Scuseria, G. E., Eds.; Elsevier: Amsterdam, 2005; p 1167.

(61) Frisch, M. J. T., G. W.; Schlegel, H. B.; Scuseria, G. E.; Robb, M. A.; Cheeseman, J. R.; Scalmani, G.; Barone, V.; Mennucci, B.; Petersson, G. A.; Nakatsuji, H.; Caricato, M.; Li, X.; Hratchian, H. P.; Izmaylov, A. F.; Bloino, J.; Zheng, G.; Sonnenberg, J. L.; Hada, M.; Ehara, M.; Toyota, K.; Fukuda, R.; Hasegawa, J.; Ishida, M.; Nakajima, T.; Honda, Y.; Kitao, O.; Nakai, H.; Vreven, T.; Montgomery, Jr., J. A.; Peralta, J. E.; Ogliaro, F.; Bearpark, M.; Heyd, J. J.; Brothers, E.; Kudin, K. N.; Staroverov, V. N.; Kobayashi, R.; Normand, J.; Raghavachari, K.; Rendell, A.; Burant, J. C.; Iyengar, S. S.; Tomasi, J.; Cossi, M.; Rega, N.; Millam, N. J.; Klene, M.; Knox, J. E.; Cross, J. B.; Bakken, V.; Adamo, C.; Jaramillo, J.; Gomperts, R.; Stratmann, R. E.; Yazyev, O.; Austin, A. J.; Cammi, R.; Pomelli, C.; Ochterski, J. W.; Martin, R. L.; Morokuma, K.; Zakrzewski, V. G.; Voth, G. A.; Salvador, P.; Dannenberg, J. J.; Dapprich, S.; Daniels, A. D.; Farkas, Ö.; Foresman, J. B.; Ortiz, J. V.; Cioslowski, J.; Fox, D. J. *Gaussian 09*, revision A.1; Gaussian, Inc.: Wallingford, CT, 2009.

(62) Roos, B. O. In *Advances in Chemical Physics*; Lawley, K. P., Ed.; Wiley Interscience: New York, 1987; p 339.

(63) Johnson, E. R.; Mori-Sanchez, P.; Cohen, A. J.; Yang, W. *J. Chem. Phys.* **2008**, *129*, 204112.

(64) Kang, J. K.; Musgrave, C. B. *J. Chem. Phys.* **2001**, *115*, 11040.

(65) Zhang, Y.; Yang, W. *J. Chem. Phys.* **1998**, *109*, 2604.

(66) Cohen, A. J.; Mori-Sánchez, P.; Yang, W. *Science* **2008**, *321*, 792.

(67) Li, H.; Pomelli, C. S.; Jensen, J. H. *Theor. Chem. Acc.* **2003**, *109*, 71.

(68) Li, H.; Jensen, J. H. *J. Comput. Chem.* **2004**, *25*, 1449.

(69) Marenich, A. V.; Cramer, C. J.; Truhlar, D. G. *J. Phys. Chem. B* **2009**, *113*, 6378.

(70) Camaioni, D. M.; Dupuis, M.; Bentley, J. *J. Phys. Chem. A* **2003**, *107*, 5778.

(71) Chipman, D. M.; Chen, F. *J. Chem. Phys.* **2006**, *124*, 144507.

(72) Chipman, D. M. *J. Chem. Phys.* **2003**, *118*, 9937.

(73) Kamerlin, S. C. L.; Haranczyk, M.; Warshel, A. *ChemPhysChem* **2009**, *10*, 1125.

(74) Ho, J.; Coote, M. L. *J. Chem. Theory Comput.* **2009**, *5*, 295.

(75) Mulliken, R. S. *J. Chem. Phys.* **1955**, *23*, 1833.

(76) Spackman, M. A. *J. Comput. Chem.* **1996**, *17*, 1.

(77) Montgomery, J. A.; Frisch, M. J.; Ochterski, J. W.; Petersson, G. A. *J. Chem. Phys.* **1999**, *110*, 2822.

(78) Winget, P.; Cramer, C. J.; Truhlar, D. G. *Theor. Chem. Acc.* **2004**, *112*, 217.

(79) Liptak, M. D.; Shields, G. C. *J. Am. Chem. Soc.* **2001**, *123*, 7314.

(80) Koch, D. M.; Toubin, C.; Peslherbe, G. H.; Hynes, J. T. *J. Phys. Chem. C* **2008**, *112*, 2972.

(81) Somani, S.; Mukhopadhyay, A.; Musgrave, C. *J. Phys. Chem. C* **2011**, *115*, 11507.

(82) Mukhopadhyay, A. B.; Musgrave, C. B. *Appl. Phys. Lett.* **2007**, *90*, 173120.

(83) Kang, J. K.; Musgrave, C. B. *J. Chem. Phys.* **2002**, *116*, 275.

(84) Bianco, R.; Hay, P. J.; Hynes, J. T. *J. Phys. Chem. A* **2011**, *115*, 8003.

(85) Mikulski, R. L.; Silverman, D. N. *Biochim. Biophys. Acta, Proteins Proteomics* **2010**, *1804*, 422.

(86) DuBois, D. L.; Bullock, R. M. *Eur. J. Inorg. Chem.* **2011**, 1017.

(87) Bonin, J.; Costentin, C.; Robert, M.; Saveant, J. M.; Tard, C. *Acc. Chem. Res.* **2012**, *45*, 372.

(88) Haake, P.; Wallerberg, G.; Boger, J. *J. Am. Chem. Soc.* **1971**, *93*, 4938.

(89) Fetter, J. R.; Qian, J.; Shapleigh, J.; Thomas, J. W.; García-Horsman, A.; Schmidt, E.; Hosler, J.; Babcock, G. T.; Gennis, R. B.; Ferguson-Miller, S. *Proc. Natl. Acad. Sci.* **1995**, *92*, 1604.

(90) Nair, S. K.; Christianson, D. W. *J. Am. Chem. Soc.* **1991**, *113*, 9455.

(91) Han, S. Y.; Chu, I.; Kim, J. H.; Song, J. K.; Kim, S. K. *J. Chem. Phys.* **2000**, *113*, 596.

(92) Bryantsev, V. S.; Diallo, M. S.; Goddard Iii, W. A. *J. Phys. Chem. B* **2008**, *112*, 9709.

(93) Borden, J.; Crans, D. C.; Florián, J. *J. Phys. Chem. B* **2006**, *110*, 14988.

(94) Kamrath, M. Z.; Relph, R. A.; Johnson, M. A. *J. Am. Chem. Soc.* **2010**, *132*, 15508.

(95) Schleyer, P. V.; Puhlhofer, F. *Org. Lett.* **2002**, *4*, 2873.

(96) Cyranski, M. K. *Chem. Rev.* **2005**, *105*, 3773.

(97) Evans, M. G.; Polanyi, M. *Trans. Faraday Soc.* **1935**, *31*, 0875.